ISSN 1023-1935, Russian Journal of Electrochemistry, 2014, Vol. 50, No. 3, pp. 208–222. © Pleiades Publishing, Ltd., 2014.
Original Russian Text © Yu.G. Chirkov, V.I. Rostokin, 2014, published in Elektrokhimiya, 2014, Vol. 50, No. 3, pp. 235–250.

Computer Simulation of Active Layers in the Electric Double Layer Supercapacitor: Optimization of Active Layer Charging Modes and Structure, Calculation of Overall Characteristics

Yu. G. Chirkov[a, z] **and V. I. Rostokin**[b]

[a] *Frumkin Institute of Physical Chemistry and Electrochemistry, Russian Academy of Sciences, Leninskii pr. 31, Moscow, 119071 Russia*

[b] *National Research Nuclear University (Moscow Engineering Physics Institute), Kashirskoe sh. 31, Moscow, 115409 Russia*

Received December 7, 2012

Abstract—The structure and functioning modes of active layers in an electric double layer capacitor (EDLC) with an aqueous electrolyte are simulated by means of a computer. A model of active layers prepared from activated carbon materials is proposed, percolation estimates are performed and effective ionic conductivities are calculated. The polarization of active layers includes a sequence of two charging processes: first, galvanostatic and then potentiostatic. The proposed program of calculations involves mutual matching and optimization of seven parameters characterizing the active layer and conditions of charging processes. According to calculations, galvanostatic polarization of wide pores in the EDLC biporous active layer up to the limiting potential followed by potentiostatic polarization of fine pores allows the capacity $C_{sp} = 246$ F/g and the energy $W_{sp} = 107$ kJ/kg to be obtained in fractions of second.

Keywords: computer simulation, electric double layer supercapacitor, galvanostatic and potentiostatic charging modes, active layer with biporous structure, activated carbon, aqueous electrolyte

DOI: 10.1134/S1023193514030033

1. PROBLEM STATEMENT

Electrochemical capacitors or simply supercapacitors that employ the electric double layer recharging processes can provide the specific capacitance of an order of magnitude of 100 F/g and the energy of 50 kJ/kg [1]. These supercapacitors are subdivided into electric double layer capacitors (EDLC), pseudocapacitors (PsC), and hybrid capacitors (HC) [2]. The present study is focused only on EDLC, in contrast to earlier studies [3, 4] which considered the effect of side reactions and faradaic processes.

An EDLC consists of two polarized porous electrodes (two active layers) immersed into either aqueous or nonaqueous electrolyte solution [5]. To obtain high EDLC characteristics, active layers with the high specific surface area of an order of magnitude of several hundred or several thousands of m^2/g (highly disperse activated carbons and tissues) are used [6–8]. Nowadays, carbon as an active electrode material is used in the majority of commercial systems (nearly 95% of the market [9]).

One of the central problems of EDLC investigations is the elucidation of the relationship between its overall characteristics and parameters of the active layer porous structure. According to IUPAC [10], the pores in active layers are characterized as follows: micropores (with diameters below 2 nm), mesopores (from 2 to 50 nm), and macropores (over 50 nm).

The relationship between overall characteristics and the structure of porous electrodes was discussed in reviews [11–14] and numerous papers. The leading role of not only micropores in active layers (they determine the high EDLC capacity and energy) but also macropores was revealed. The contribution of the latter is negligible but they provide the transport of ions to the charged surfaces and can enhance the EDLC power.

The final conclusion that stems from these studies is as follows. Acknowledging a certain role of mesopores and understanding that not the whole micropore surface found by well-known adsorption methods (BET, etc.) may be accessible for charging of the double layers in it, it should be assumed that for the optimal functioning of EDLC active layers made of activated carbon materials, the balance should be observed between contributions of micro and macropores in the size distribution of pores, i.e., their average sizes should be correctly chosen.

The analysis of functioning of EDLC active layers can be carried out either by impedance (transmission lines) methods proposed by de Levie [15, 16] or by solving systems of equations describing physical pro-

[z] Corresponding author: olga.nedelina@gmail.com (Yu.G. Chirkov).

cesses in EDLC active layers [17, 18]. In the present study, the second way is taken.

This study is aimed at computer simulation of the structure and functioning of EDLC active layers made of highly disperse activated carbon by subjecting them first to galvanostatic and then to potentiostatic charging and also at the development of a method for calculating overall characteristics, namely, the specific capacitance and the energy.

2. THE CENTRAL PROBLEM OF EDLC

Carbon materials find the progressively wider practical application. Activated carbons are synthesized by carbonization of organic substances or fossil carbons (synthesis of a product with the high carbon content). The next stage is the activation process during which the porosity develops further and micropores become more accessible [20].

For an EDLC, it is important to combine micropores with meso and macropores. In the further consideration, to avoid unnecessary complications of the EDLC model, we assume that mesopores are absent and we have only micro and macropores.

The galvanostatic mode of EDLC charging would seem capable of quickly providing the high values of specific capacitance and energy. Actually, this is associated with complications. In [21], the parameter τ was introduced. It means the characteristic time of charging of the surface of a porous structure and takes the form

$$\tau = SC_sL^2/\kappa, \quad (1)$$

where S (cm^{-1}) is the specific surface to be charged; C_s (F/cm^2) is the specific capacitance of the electric double layer, L (cm) is the active layer thickness, κ ($S\ cm^{-1}$) is the effective specific conductivity of ions in the active layer.

The surface area S is inversely proportional to the pore size (radius or diameter) ρ

$$S \sim 1/\rho. \quad (2)$$

Hence, if the radius of wide pores ρ_2 much exceeds the radius of fine pores ρ_1, then, according to definition (1), the characteristic time for charging the wide pores τ_2 turns out to be far smaller than the characteristic time it takes to charge the fine pores τ_1. Thus, we have the inequality

$$\tau_2 \ll \tau_1. \quad (3)$$

It means that at galvanostatic charging, the wide pores are first to be polarized and only after this, the polarization of finer pores is possible. However, the charging process can be carried out only up to a certain moment. The potential E of the surface being charged in the active layer cannot exceed a certain limit E^*. Thus, in aqueous electrolyte solutions at polarization of activated carbon, the potential deviates from its initial value $E^* - E_0 \sim 1$ V.

Table 1. Dependence of EDLC charging time t^* (potentiostatic conditions) on the active layer thickness L

L, cm	t^*, s
0.01	0.675
0.1	67.5
1	6.75×10^3

The presence of wide pores in active layers is a result of using technologies for synthesizing activated carbons. The wide pores open access to finest pores and, seemingly, should enhance the EDLC characteristics. But the same wide pores that are polarized so quickly become an obstacle to charging micropores in the galvanostatic mode. The high overall characteristics cannot be reached. This is the central problem for EDLC.

Supercapacitors can be charged by means of a potentiostat by setting the limiting potential value E^*. However, in this case, their charging is a relatively long process. The time of active layer charging t^* can be assessed by solving the following equation:

$$E(0,t^*) = E^* - (E^* - E_0)\frac{4}{\pi}\sum_{m=0}^{\infty}\frac{(-1)^m}{2m+1} \times \exp\left\{-\left(\frac{\pi(2m+1)}{2}\right)^2\frac{t^*}{\tau}\right\} = \eta E^*. \quad (4)$$

Let us assume that the active layer consists of a uniform ultradisperse material containing micropores with the radius of an order of magnitude of 1 nm. Here, $E(0, t^*)$ is the potential at the back surface of the active layer. Assume that $E_0 = 0.5$ V and $E^* = 1.5$ V; $\tau = SC_sL^2/\kappa$ is the aforementioned characteristic time of charging.

Assume $S = 1.359 \times 10^7\ cm^{-1}$, $C_s = 2 \times 10^{-5}\ F/cm^2$, $\kappa = 0.11\ S\ cm^{-1}$ [21]. Furthermore, assume that the increasing potential in the active layer reaches $E(0, t^*) = 0.999\ E^*$. Table 1 shows the results of calculations of t^*. It is evident that the charging of active layers with the thickness $L \sim 0.1-1$ cm takes several tens of minutes rather than several seconds.

Thus, taken separately, neither galvanostatic nor potentiostatic modes of EDLC charging allow specific capacitance of several hundred of F/g to be reached in several seconds or even several fractions of second.

The central problem of EDLC can be solved by dividing the charging process into two stages: first, in the galvanostatic mode, the surface of wide pores is charged up to the maximum permissible value E^* and then the charging is continued in the potentiostatic mode by establishing the potential $E = E^*$. However, several questions arise and the present study is to answer them.

First, for a given average radius of fine pores ρ_1, we must find the optimal average radius of wide pores ρ_2.

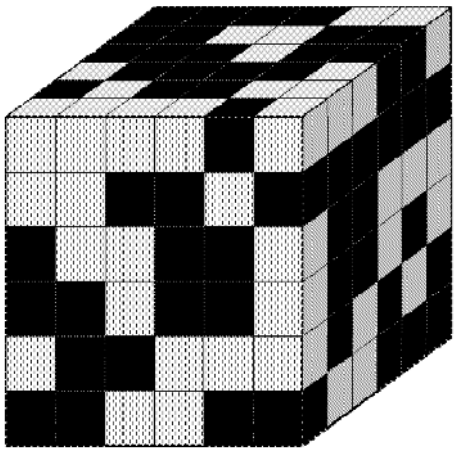

Fig. 1. Illustration of a model the active layer structure for a biporous EDLC (model of equal-sized cubic grains of two types). Black cubes are porous carbon grains, light cubes are electrolyte grains: $g = 0.5$.

Furthermore, the optimal ratio of the highly disperse active layer part g should be specified.

Second, in the first stage of charging (galvanostatic), the correct choice of the following two parameters is important: the active layer thickness L and the charging current (galvanostatic charging) I.

Third, the galvanostatic process (its time is designated as t_{gal}) should proceed much quicker as compared with the potentiostatic process (its time is designated as t_{pot}). The condition $t_{gal} \ll t_{pot}$ should be observed.

Fourth, the optimal time consumed in polarization of fine pores under potentiostatic conditions should be determined, because the flow of ions to fine pores weakens and vanishes at the infinite charging time.

Fifth, it is desirable to know what values of capacitance and energy can be realized when using the two-step process of EDLC charging.

Thus, the program of calculations implies the mutual matching and optimization of seven parameters: ρ_1, ρ_2, g, L, I, t_{gal}, t_{pot}. Now we embark on realization of this calculation program.

Yet another note. This study is carried out within the framework of computer-assisted simulations. Computer simulations are a separate and well-developed field which has its own principles, approaches, apparatus, requires good physical and mathematical education, the knowledge of high-level computer languages, etc. In essence, its goal is to supplement experimental studies and even plan the latter.

3. COMPUTER MODEL OF ACTIVE LAYER STRUCTURE

Active layers represent the most important component of many types of electrochemical devices: fuel cells, electrolyzers, electrosynthetic cells, lithium-ion batteries, supercapacitors, etc. To obtain high overall currents or work out a sufficient amount of the target product, it is first of all necessary to optimize the channels in the active layer for the continuous delivery of ions and electrons to the catalyst surface.

The program of computer simulations of active layers in electrochemical technology of one or another type consists of a sequence of successive steps:

(1) development of a computer model of the active layer structure;

(2) investigation of percolation properties of this computer model;

(3) determination of effective coefficients of the active layer (these coefficients are involved in equations describing the processes in the active layer);

(4) calculation of the major overall characteristics of the active layer;

(5) if required, optimization of functioning of the active layer under study.

The ultimate goal of studying the biporous active layer of EDLC is to calculate the overall characteristics of the assumed active layer structure, namely, the charging time and the specific values of capacitance and energy.

Figure 1 shows the model of an EDLC biporous active layer. Here, the electrolyte-filled coarse pores-voids are randomly mixed with agglomerates of numerous fine carbon particles on the surface of which the charge should generally be adsorbed.

Below, the electrolyte-filled voids and electrolyte-wetted agglomerates of fine carbon particles are called the "grains", i.e., electrolyte grains and carbon grains, respectively. Assume that these grains and equal-sized and shaped as cubes with edge D. In this model, the fine carbon particles which partly occupy the volume of carbon grains are also represented as microcubes with equal edge d. Thus, to describe the structure of the EDLC active layer, we have assumed the biporous model of equal-sized grains of two types. Figure 1 illustrates this model. It is evident, that the following relationship is observed:

$$g + g_i = 1, \tag{5}$$

where g is the volume concentration (fraction) of porous carbon grains (the main parameter), g_i is the volume concentration (fraction) of electrolyte grains.

The three-dimensional model of the EDLC active layer is chosen to be a model cube with dimensions of $N_s \times N_s \times N_s = N_s^3$. The model cube should have macroscopic dimensions. This means that as in real cases, the active layer thickness L much exceed the size of individual grains D. The following inequality should be observed:

$$D \ll L. \tag{6}$$

The point is that as was shown in [22], the percolation characteristics of the porous medium become stable and undergo no changes upon the attainment of

sufficiently large values of parameter N_s. This can be achieved by assuming $N_s = 100$. In the further consideration, the model cube under study accommodates $100 \times 100 \times 100 = 10^6$, i.e., a million of grains of both types.

4. PERCOLATION CHARACTERISTICS OF THE ACTIVE LAYER

The second stage of computer simulations consists of percolation estimates.

In the active layer, two percolation clusters should be distinguished [23], ionic (electrolyte grains) and electronic (carbon grains) clusters. Each of these clusters represents a combination of interconnected grains of one or another type. Percolation clusters uniformly transpierce the total active layer thickness.

Percolation clusters are formed when the percolation threshold is reached, in other words, when the volume concentrations of the corresponding grains reach their critical values, i.e., g^{***} or g_i^{***}. In the cubic lattice of sites [23] under consideration, the percolation threshold, as was demonstrated in [24], is equal to

$$g^{***} = g_i^{***} = [(1 + 2^{1/2})^{1/3} + (1 - 2^{1/2})^{1/3}]/2 = 0.298. \quad (7)$$

Thus, for functioning of the active layer, at least the following two conditions should be fulfilled:

$$g \geq 0.30, \quad g_i \geq 0.30. \quad (8)$$

Conditions (5) and (8) mean that the fraction of carbon grains should be localized in the interval

$$0.3 \leq g \leq 0.7, \quad (9)$$

if we assume that ions enter the active layer mainly via electrolyte grains and electrons enter it via carbon grains.

Now, a significant note should be made. As was shown in [25], the true percolation clusters appear at neither $g^{***} = 0.298$ nor $g_i^{***} = 0.298$ but at the higher concentrations, i.e., $g \geq 0.35$ and $g_i \geq 0.35$. At the lower values, the clusters are only being developed and occupy a small part of the model cube volume. Hence, it is reasonable to consider the narrower interval of permissible concentrations g and g_i

$$g \geq 0.35, \quad g_i \geq 0.35. \quad (10)$$

Thus, the working interval of carbon grains in the active layer is limited by inequalities

$$0.35 \leq g \leq 0.65. \quad (11)$$

Now, we carry out computer calculations (its results are necessary for the further consideration) of the dependences of the normalized specific surface of contact between two percolation clusters (electronic and ionic) S^* on the volume concentration (fraction) of carbon grains g. Table 2 shows the results of calculations.

Table 2. EDLC active layer: dependence of the specific contact surface between two percolation clusters (electronic and ionic) S^* on the volume concentration of carbon grains g

g	S^*
0.35	0.885
0.40	1.189
0.45	1.320
0.50	1.359
0.55	1.320
0.60	1.189
0.65	0.885

The value S^* reaches its maximum at $g = 0.5$. In this point, the electronic and ionic percolation clusters are equivalent and closely intertwined. The specific surface of the contact between two types of clusters S^{**} (cm^2/cm^3) can be calculated by the formula

$$S^{**} = S^*/D. \quad (12)$$

5. CALCULATIONS OF THE EFFECTIVE SPECIFIC IONIC CONDUCTIVITY

To calculate the overall characteristics of EDLC, we need to know the effective ionic conductivity (the third stage of computer simulations). It should be noted once more that ionic conduction is typical of not only electrolyte grains but also carbon grains because the latter are only partly filled with carbon particles and their remaining volume is impregnated with electrolyte.

Algorithms for computer calculations of the effective ionic conductivity can be found in [25, 26]. Here, the following should be noted. First of all, the object of our primary interest is naturally carbon grains with the high specific surface. Hence, the edge of carbon microcubes d in carbon grains should be assumed to be sufficiently small, i.e., the following inequality should be fulfilled:

$$d \ll D. \quad (13)$$

Second, an analogy is evident between the distribution of carbon grains and electrolyte grains in the active layer and the distribution of carbon microcubes and electrolyte-filled microcubes-voids in individual carbon grains. The specific surface area of carbon microcubes in carbon grains can be assessed by the formula

$$S = S^*/d. \quad (14)$$

The value of S^* can be taken from Table 1 by substituting the volume concentration of carbon microparticles in carbon grains g^{**} for g.

It is desirable that the specific surface area S in Eq. (14) is the maximum. Hence, in further consider-

Table 3. Carbon grains: dependence of the normalized effective ionic conductivity κ^* on the volume concentration of carbon particles g^{**}

g^{**}	κ^*
0.35	0.295
0.40	0.230
0.45	0.171
0.50	0.110
0.55	0.060
0.60	0.026
0.65	0.005

Table 4. Dependence of the normalized specific ionic conductivity of the EDLC active layer κ^{**} on the volume concentration of carbon grains g for $g^{**} = 0.5$

g	κ^{**}
0.3	0.552
0.4	0.430
0.5	0.346
0.6	0.268
0.7	0.206
0.8	0.155
0.9	0.129
1.0	0.110

ation we assume that $g^{**} = 0.5$ and in Eq. (14) $S^* = 1.359$ (data of Table 1).

Table 3 shows the results of calculations of the dependence of the effective ionic conductivity κ^* on the concentration of carbon particles (carbon microcubes) g^{**} [21]. The conductivity κ^* quickly drops with the increase in g^{**}. Note that for the optimal concentration $g^{**} = 0.5$, the effective specific conductivity is shown to be $\kappa^* = 0.11$.

What remains is to estimate the dependence of the effective specific ionic conductivity κ^{**} of the active layer on the concentration of carbon grains g. The active layer consists of a mixture of electrolyte grains with the conditional conductivity equal to 1 and also of carbon grains with the conditional conductivity κ^* (Table 3). Table 4 shows the results of calculations.

In was assumed that $g^{**} = 0.5$ [21]. It is obvious that for $g = 1.0$ (the active layer consists only of carbon grains), $\kappa^{**} = 0.11$. Ultimately, the effective value of the specific ionic conductivity of the active layer κ can be determined by the obvious formula

$$\kappa = \kappa_0 \kappa^{**}, \quad (15)$$

where κ_0 is the specific ionic conductivity of the electrolyte chosen.

6. GALVANOSTATIC CHARGING

The fourth stage of computer simulations of the EDLC active layer consists of calculations of overall characteristics. We divide the charging processes into two steps: first of all we charge galvanostatically the surface of wide pores to reach the limiting value E^* and then we continue the charging of fine pores under potentiostatic conditions by fixing the potential at $E = E^*$.

The galvanostatic mode was studied in detail in [21] for various versions of the active layer structure. There, the overall EDLC characteristics were calculated by approximate formulas. It was assumed that the charges that enter into the active layer volume are uniformly distributed throughout the active layer thickness. This is why the potential value in the active layer is virtually uniformly distributed throughout its thickness in all moments.

It is useful to compare the results of calculations according approximate [21] and exact (Appendix 1) formulas. Figure 2 shows that time dependence of the specific volume capacitance. The capacitance values differ both at small charging times and especially in the end of the galvanostatic process. This is associated with the fact that the active layer thickness is assumed to be large, $L = 1$ cm. Hence, one cannot speak of equal accessibility of the active layer thickness with respect to charge and potential. This is why one has to operate with exact formulas.

Figure 3 shows what happens when L decreases. As the active layer thickness changes from $L = 1$ cm (curves *3*, *3*') to $L = 10^{-2}$ cm (curves *1*, *1*'), the layer acquires equal accessibility as regards both charge and potential so that the approximate and the exact formulas produce the same result.

Now, the EDLC active layer is charged in the galvanostatic mode by taking different values of charging current I and active layer thickness L. Table 5 shows the results of calculations (accomplished according to formulas shown in Appendix 1).

The galvanostatic charging of the surface of coarse pores can provide only small values of capacitance and energy. However, galvanostatics makes it possible to quickly increase the potential on the coarse pore surface up to its limiting value. Moreover, it can be assumed that the charging of fine pores has not yet started.

We assume that the galvanostatic process is stopped. Then, the limiting potential is maintained and the process of potentiostatic charging starts. In the process, the charge migrates from coarse pores to fine pores. The inner surface of carbon grains is charged which increases the EDLC capacitance and the energy. Let us consider in detail how to calculate this increase.

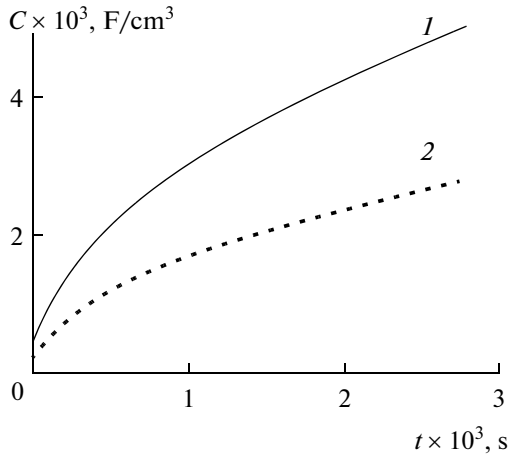

Fig. 2. Galvanostatic charging. Dependence of the specific volume capacitance C_{sp} on the time t. Comparison of (*1*) exact and (*2*) approximate calculations. $L = 1$ cm. $E_0 = 0.5$ V, $E^*(L) = 1.5$ V, $g = 0.65$, $g_i^* = 0.25$, $\kappa_0 = 0.8$ S cm^{-1}, $\kappa = 0.2$ S cm^{-1}, $D = 10^{-3}$ cm, $S = 8.85 \times 10^2$ cm^{-1}, $C_s = 2 \times 10^{-5}$ F/cm^2.

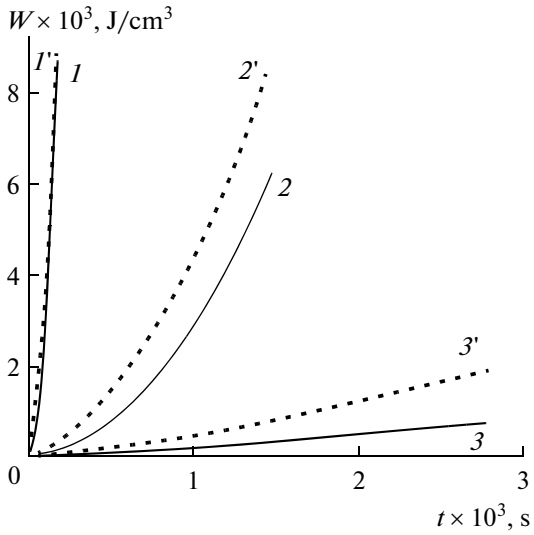

Fig. 3. Galvanostatic charging. Dependence of the specific volume energy W_{sp} on the time t for three thickness values L of the EDLC active layer. Comparison of (*1–3*) exact and (*1'–3'*) approximate calculations. L, cm: (*1*, *1'*) 10^{-2}, (*2*, *2'*) 10^{-1}, (*3*, *3'*) 1. $E_0 = 0.5$ V, $E^*(L) = 1.5$ V, $g = 0.65$, $g_i^* = 0.25$, $\kappa_0 = 0.8$ S cm^{-1}, $\kappa = 0.2$ S cm^{-1}, $D = 10^{-3}$ cm, $S = 8.85 \times 10^2$ cm^{-1}, $C_s = 2 \times 10^{-5}$ F/cm^2.

7. MODEL OF CYLINDRCAL ELECTROLYTE PORES

First of all, it is expedient to cut the model cube (Fig. 1) by a plane parallel to its front and back surfaces and then elucidate using a computer how carbon and electrolyte grains are distributed in this particular section (Figs. 4a and 4b).

In Figs. 4a and 4b, the carbon grains involved in the electronic cluster are marked black and the electrolyte grains involved in the ionic cluster are marked gray. In Fig. 4a, the concentration of carbon grains is extremely small according to condition (11), because here $g = 0.35$ while the concentration of electrolyte grains is the maximum ($g_i = 0.65$). In contrast, in Fig. 4b, the concentration of carbon grains is the maximum because here $g = 0.65$ while the concentration of electrolyte grains is extremely low ($g_i = 0.35$). Figure 4a shows a well developed electrolyte (ionic) percolation cluster, whereas the electronic cluster built of carbon grains is weakly developed so only its parts are seen in the present section. Figure 4b shows the opposite case.

In Fig. 4a within the electrolyte cluster, some inclusions are marked white. These are carbon grains isolated from the electronic clusters. They are not feed with electrons and cannot be charged. In Fig. 4b, in the electronic cluster, electrolyte grains isolated from the ionic cluster are seen; they dilute the concentration of carbon grains in the electronic cluster.

It is virtually impossible to calculate the final result of charging processes by using data of Figs. 4a and 4b; moreover, the pattern of grain distribution in other sections of the active layer model cube (Fig. 1) should be different. Hence, in calculations it is expedient to rely on parameters which remain unchanged in the model cube and depend only on parameter g.

These invariants can be the specific contact surface between electronic and ions clusters S^* (data of Table 2) and four more parameters: the fractions of grains involved in the electronic cluster g^* and grains isolated

Table 5. EDLC, galvanostatic charging, aqueous electrolyte: dependences of the charging time t, the specific capacitance C/L and the specific energy W/L on the charging current I and the active layer thickness L. The initial potential $E_0 = 0.5$ V, the maximum possible potential $E^*(L) = 1.5$ V, $g = 0.65$, $g_i^* = 0.25$, $\kappa_0 = 0.8$ S cm^{-1}, $\kappa = 0.2$ S cm^{-1}, $D = 10^{-3}$ cm, $S^{**} = 8.83 \times 10^2$ cm^{-1}, $C_s = 2 \times 10^{-5}$ F/cm^2

I, A/cm^2	L, cm	$t \times 10^3$, s	C/L, F/cm^3	$(W/20) \times 10^3$, J/cm^3
1.0	0.001	0.177	0.177	8.82
	0.01	1.740	0.177	8.56
	0.1	14.750	0.176	6.19
0.1	0.001	1.770	0.177	8.85
	0.01	17.700	0.177	8.82
	0.1	174.000	0.177	8.56
0.01	0.001	17.700	0.177	8.85
	0.01	177.000	0.177	8.85
	0.1	1770.000	0.177	8.82

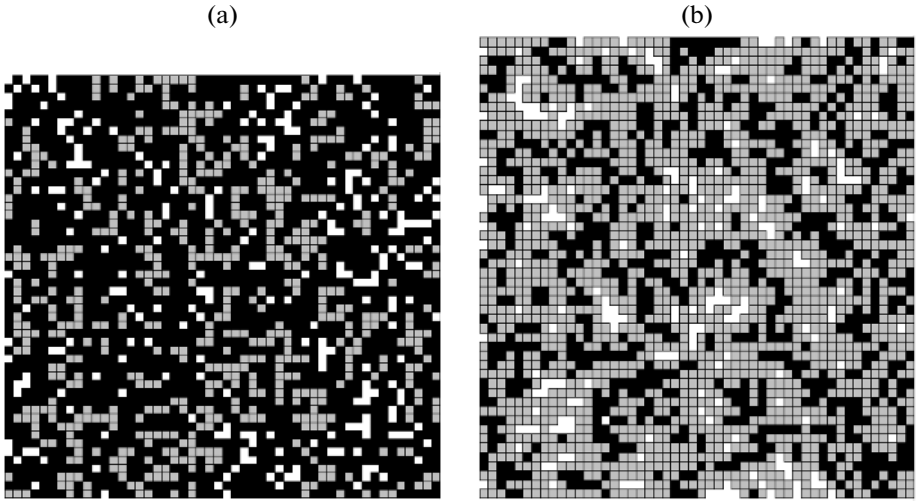

Fig. 4. An arbitrary section of the model cube by a plane parallel to its front and back sides. Carbon grains (black) and electrolyte grains (grey) for $g = 0.35$ (Fig. 4a) and $g = 0.65$ (Fig. 4b). Isolated grains uninvolved in electronic clusters (Fig. 4a) or isolated electrolyte grains uninvolved in the ionic cluster (Fig. 4a) are white.

from the latter $g - g^*$ and also the fractions of grains involved in the electrolyte cluster g_i^*, and those isolated from the latter $g_i - g_i^*$. Due to the chosen dimensions of the model cube, all these values remain constant irrespective of section. Table 6 shows the calculated dependences of these four parameters on the major parameter g.

Now, we proceed to ordering the elements involved in the active layer. Let us create a regular structure equivalent to those exemplified in Figs. 4a and 4b. We call this structure the model of cylindrical electrolyte pores.

Assume that pores are parallel to one another, distributed uniformly in the active layer, and perpendicular to the active layer front surface to form a square network on this surface. The material for these pores includes grains involved in the electrolyte cluster (their fraction is g_i^*) and carbon grains isolated from the electronic cluster (their fraction is $g - g^*$) which are integrated into the ionic cluster (Fig. 4a). The total external specific surface of electrolyte pores is determined as S^*/D.

Table 6. Dependence of the major parameters of ionic and electronic percolation clusters on the concentration (fraction) of carbon grains g

g	g^*	$g - g^*$	g_i	g_i^*	$g_i - g_i^*$
0.35	0.25	0.10	0.65	0.649	0.001
0.40	0.35	0.05	0.60	0.597	0.003
0.45	0.43	0.02	0.55	0.54	0.01
0.50	0.49	0.01	0.50	0.49	0.01
0.55	0.54	0.01	0.45	0.43	0.02
0.60	0.597	0.003	0.40	0.35	0.05
0.65	0.649	0.001	0.35	0.25	0.10

In further consideration, we need two more invariants. First of all, this is

$$g_i^{**} = g_i^* + (g - g^*) \quad (16)$$

the fraction of electrolyte grains involved in the electrolyte cluster plus the fraction of carbon grains "stuck" in this cluster (i.e., isolated carbon grains). This combination is called the fraction of grains involved in the effective electrolyte cluster.

Secondly, we are interested in the degree of dilution of the electronic cluster, i.e., the fraction of carbon grains involved in the electronic cluster divided by the sum of these carbon grains plus electrolyte grains integrated into the electronic cluster. We designate this value as α, it is determined as

$$\alpha = g^*/[g^* + (g_i - g_i^*)]. \quad (17)$$

Table 7 shows the dependence of α and g_i^{**} on g.

The major parameters of the model of cylindrical electrolyte pores should be determined based on the following sufficiently obvious relationships:

$$g_i^{**} = \pi(R)^2 n, \quad (18)$$

$$S^*/D = 2\pi R n, \quad (19)$$

where R is the cylindrical pore radius, n is the number of electrolyte pores per cm^2 of the active layer surface, S^* is the normalized specific surface of the contact of an electrolyte cluster with an electronic cluster, D is the edge of small cubes inside the model cube.

It follows from the system of equations (18) and (19) that

$$R/D = 2g_i^{**}/S^*, \quad (20)$$

$$nD^2 = (S^*/2)^2/\pi g_i^{**}, \quad (21)$$

$$l/D = 1/2Dn^{1/2} = (\pi g_i^{**})^{1/2}/S^*, \quad (22)$$

$$R/l = 2(g_i^{**}/\pi)^{1/2}, \quad (23)$$

where l is the half-distance between the neighboring cylindrical pores. Table 8 demonstrates all parameters of the model of cylindrical electrolyte pores.

8. PARAMETERS OF HIGHLY DISPERSE LAYERS

Now we embark on the second stage of charging of a biporous EDLC, i.e., to potentiostatic conditions. In the model proposed, it is the highly disperse layer adjacent to each electrolyte pore and bounded by two cylindrical surfaces with the polar radii $r_1 = R$ and $r_2 = l$ that is charged. This layer is formed by not only carbon grains but also electrolyte grains isolated from the electrolyte cluster. The formulas that describe the migration of ions to carbon grains surrounding cylindrical electrolyte pores can be found in Appendix 2. The carbon medium that surrounds electrolyte pores is assumed to be homogeneous and characterized by effective parameters κ^{***} and S^{***}. Let us determine these parameters.

Assume that the concentration of carbon grains in the active layer is $g = 0.65$. Then, the mixture of carbon grains and isolated electrolyte grains in the highly disperse layer corresponds to $g + (g_i - g_i^*) = 0.65 + 0.10 = 0.75$ (see data in Table 6). The fraction of carbon grains in the mixture is $g = 0.65/0.75 = 13/15 = 0.87$. Using the data in Table 4, we find that the concentration of 0.87 corresponds to the conductivity $\kappa^{**} = 0.135$. Hence, $\kappa^{***} = 0.8 \times 0.135 = 0.108$ S cm^{-1}, where $\kappa_0 = 0.8$ S cm^{-1} is the aqueous electrolyte conductivity. The specific surface of carbon in the mixture of carbon grains and isolated electrolyte grains is $S^{***} = 1.359 \times 10^7 \times 0.87 = 1.18 \times 10^7$ cm^{-1}. Table 9 shows the same estimates for the other g values.

9. OVERALL CHARACTERISTICS OF THE EDLC ACTIVE LAYER

Now, we calculate the overall characteristics of the EDLC active layer. First of all, we find the potential distribution along the thickness of the highly disperse layer in different moments (Fig. 5). Assume that $g = 0.65$, the grain size $D = 10^{-3}$ cm, and the potential on the back side of the highly disperse layer (at polar radius $r = l$) reaches 90% of the maximum possible value ($\eta = 0.9$).

Table 7. Dependences of the degree of dilution of the carbon material in the electronic cluster α and the fraction of grains involved in the effective electrolyte cluster g_i^{**} on the fraction of carbon grains in the model cube

g	α	g_i^{**}
0.35	0.996	0.749
0.40	0.992	0.647
0.45	0.977	0.542
0.50	0.974	0.500
0.55	0.964	0.440
0.60	0.923	0.353
0.65	0.866	0.251

Table 8. Parameters of the model of cylindrical electrolyte pores

g	R/D	nD^2	l/D	R/l
0.35	1.693	0.083	1.733	1.024
0.40	1.088	0.174	1.199	1.102
0.45	0.821	0.256	0.989	1.204
0.50	0.736	0.294	0.922	1.253
0.55	0.667	0.315	0.891	1.336
0.60	0.594	0.319	0.886	1.492
0.65	0.567	0.248	1.003	1.769

Table 9. Highly disperse layer: dependences of the effective ionic conductivity κ^{***} and the specific surface S^{***} on the fraction of carbon grains in the active layer g

g	κ^{***}, S cm^{-1}	S^{***}, cm^{-1}
0.65	0.108	1.18×10^7
0.55	0.092	1.31×10^7
0.45	0.0896	1.33×10^7
0.35	0.088	1.355×10^7

The potential is fixed at the front side of the highly disperse layer ($E^* = 1.5$ V) but quickly increases from the value E_0 at its back side. The charging time is small $t_{pot} = 5.317 \times 10^{-4}$ s. Let us compare this time with the times of galvanostatic charging t_{gal} shown in Table 5. The inequality

$$t_{gal} \ll t_{pot} \quad (24)$$

should be fulfilled.

Data in Table 5 suggest that inequality (24) is true only for certain combinations of values of the two main parameters, namely, the current I and the active layer thickness L. If, for example, we take the current $I = 1$ A/cm^2 (Table 5, lines 2–3), then, strictly speaking, the inequality (24) is fulfilled only for thin active layers with $L \le 10$ μm.

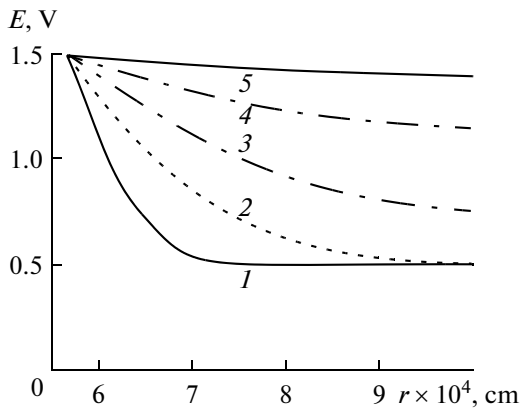

Fig. 5. Distribution of potential E throughout the thickness of the EDLC highly disperse layer at different time t. t (the fractions of the total charging time $t^* = 5.317 \times 10^{-4}$ s are shown): (*1*) 0.01, (*2*) 0.05, (*3*) 0.2, (*4*) 0.5, (*5*) 1.0. $g = 0.65$, $D = 10^{-3}$ cm, $\kappa_0 = 0.8$ S cm^{-1}, $\kappa^{***} = 0.108$ S cm^{-1}, $S^{***} = 1.18 \times 10^7$ cm^{-1}, $C_s = 2 \times 10^{-5}$ F/cm^2, $r_1 = R = 5.67 \times 10^{-4}$ cm, $r_2 = l = 1.003 \times 10^{-3}$ cm, $E_0 = 0.5$ V, $E^*(L) = 1.5$ V, $\eta = 0.9$.

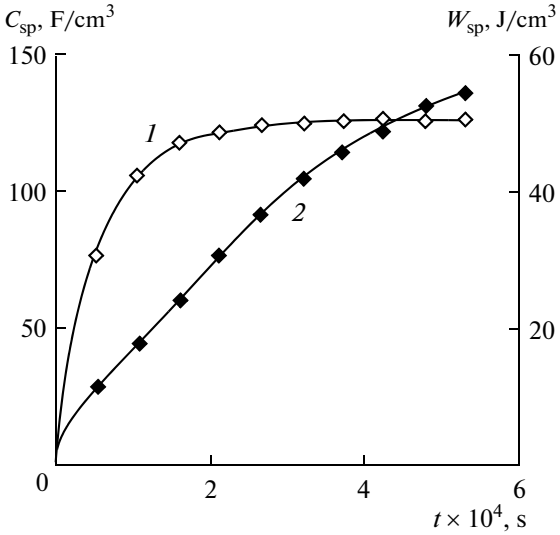

Fig. 6. Biporous EDLC active layer: dependence of specific volume values of (*1*) capacitance C_{sp} and (*2*) energy W_{sp} on time t, s. $g = 0.65$, $D = 10^{-3}$ cm, $\kappa_0 = 0.8$ S cm^{-1}, $\kappa^{***} = 0.108$ S cm^{-1}, $S^{***} = 1.18 \times 10^7$ cm^{-1}, $C_s = 2 \times 10^{-5}$ F/cm^2, $r_1 = R = 5.67 \times 10^{-4}$ cm, $r_2 = l = 1.003 \times 10^{-3}$ cm, $n = 2.48 \times 10^5$ cm^{-2}, $E_0 = 0.5$ V, $E^*(L) = 1.5$ V.

This situation can be improved by increasing the current by one order of magnitude. For $I = 10$ A/cm^2, we can deal with thicker active layers ($L \le 100$ μm). On the other hand, it is not necessary to considerably increase the charging current density in order to operate with thicker active layers ($L \ge 1$ mm). It is possible to increase the size of coarse (electrolyte) pores in our biporous model (Fig. 1), i.e., increase the edge D of cubic grains in the EDLC active layer and keep unchanged the size of fine pores.

If assume that $D = 10^{-4}$ cm, then, according to calculations ($g = 0.65$, $\eta = 0.9$), the time t_{pot} decreases to 5.317×10^{-6} s because as compared with the case of $D = 10^{-3}$ cm, the thickness of the polarized highly disperse layer drops by nearly one order of magnitude. On the other hand, assuming $D = 10^{-2}$ cm, we obviously obtain the value 5.317×10^{-2} s. Then, as follows from data in Table 5, for the galvanostatic process, the charging current density I can be taken equal to not only 1 but also 0.1 A/cm^2.

Everything mentioned above points to the importance of correct fitting and optimization of seven major parameters of the system under study, namely, ρ_1, ρ_2, g, L, I, t_{gal}, t_{pot}.

Table 10. Dependence of parameters of the highly disperse layer on the degree of charging η

η	t^*	C_{sp}	W_{sp}
0.9	5.317×10^{-4}	125.728	54.367
0.99	1.022×10^{-3}	125.846	62.042
0.999	1.513×10^{-3}	125.847	62.842

Now we consider how the overall characteristics of highly disperse layers (the contribution of coarse pores into the EDLC surface charging is neglected, being very small) increase in time together with virtually the active layer characteristics. The calculations were carried out according to formulas in Appendix 2. Figure 6 shows the results (we still assume that $g = 0.65$, $D = 10^{-3}$ cm, $\eta = 0.9$). The ultimate values of capacitance $C_{sp} = 125.7$ F/cm^3 and energy $W_{sp} = 54.4$ J/cm^3.

The above calculations were carried out under the assumption that 90% of the maximum possible potential value E^* (parameter $\eta = 0.9$) is reached on the surface of highly disperse layers with the polar radius $r_2 = l$. Now we consider how the time of potentiostatic charging and the overall parameters of EDLC change with the increase in parameter η. Table 10 shows the results of corresponding calculations. It is seen that the as the charging time increases 3-fold, the capacitance remains virtually unchanged but the energy somewhat increases.

The goal of this study was also to find the optimal value of parameter g, i.e., the fraction of carbon grains. It was shown above that the values $g > 0.65$ cannot be taken because there is no full-fledged electrolyte cluster in this region so that the proposed method of EDLC charging ceases to work. At the same time, how do the EDLC overall parameters change as we decrease the parameter g? The answers to this question can be found in Fig. 7 and Table 11.

Figure 7 shows the dependences of the specific volume capacitance C_{sp} and energy W_{sp} on the fraction of carbon grains g. It is seen that the concentration of carbon grains $g = 0.65$ should be preferred. This is associated not only with the fact that in this point the concentration of carbon grain is the maximum. Table 11 shows how the totality of the other five parameters involved in calculations changes with the decrease in g.

There is another way of assessing the maximum values of C_{sp} and W_{sp}. We tentatively assume that the carbon density is 2.2 g/cm^3. Then in terms of the model chosen with $g = 0.65$ and taking into account that the volume concentration of carbon particles in carbon grains $g^{**} = 0.5$, we obtain that the density of carbon contained in the model cube is equal to $2.2 \times 0.65 \times 0.5 = 0.715$ g/cm^3. In this case specific capacitance of of EDLC $C_{sp} = 175.8$ F/g, and specific energy $W_{sp} = 76.41$ J/g.

Furthermore, it should be taken into account that the model of cylindrical electrolyte pores does not cover the whole volume of the active layer. The potentiostatic calculations involve only a part of each cm^3 of the active layer, equal to $\pi(l^2 - R^2)$. The uninvolved surface area is equal to $(4 - \pi)l^2$. Certainly, this highly disperse part of the active layer is quickly charged too. Hence, the sum of these volumes $\pi(l^2 - R^2) + (4 - \pi)l^2 = 4l^2 - \pi R^2$ turns out to be polarized.

Let us carry out a simple extrapolation. Assume that the capacitance and energy values are proportional to the total highly disperse part of the active layer. Then the capacitance and energy values shown in Table 11 (the first line) should be multiplied by the coefficient of gain of the highly disperse part of the active layer $\psi = [4l^2 - \pi R^2]/[\pi (l^2 - R^2)]$. For $g = 0.65$ and $D = 10^{-3}$ cm, the coefficient $\psi = 1.4$. Hence, the really obtained capacitance and energy in the EDLC are $C_{sp} = 246$ F/g and $W_{sp} = 107$ J/g.

As it should be expected, the found capacitance value coincides almost exactly with its maximum possible value calculated by the simple formula $gSC_s = 0.65 \times 1.359 \times 10^7 \times 210^{-5}/0.715 = 247$ F/g.

10. CONCLUSIONS

One of the most important advantages of supercapacitors is their fast charging, in several seconds.

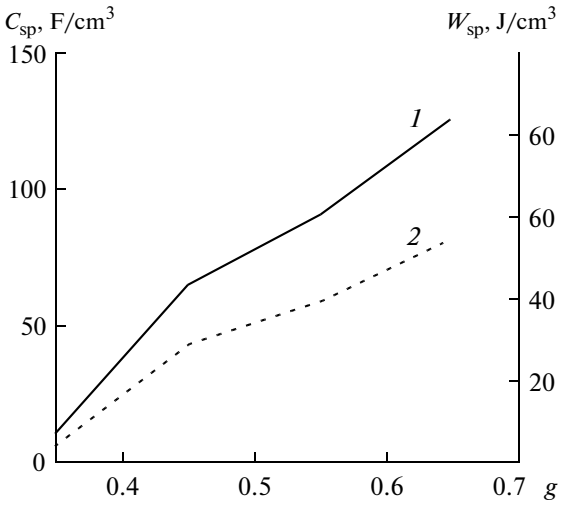

Fig. 7. Biporous EDLC active layer: dependence of the specific volume values of (*1*) capacitance C_{sp} and (*2*) energy W_{sp} on the fraction of carbon grains g. $D = 10^{-3}$ cm, $\kappa_0 = 0.8$ S cm^{-1}, $C_s = 2 \times 10^{-5}$ F/cm^2, $E_0 = 0.5$ V, $E^*(L) = 1.5$ V.

Hence, the supercapacitor active layers should be charged in the galvanostatic mode, because here the charging rate rapidly increases with the increase in the charging current density. However, this way is associated with certain complications.

The materials for active layers usually represent activated carbon. The technology of these materials is characterized by the presence of not only micropores capable of providing high capacitances but also macropores. Having the small specific surface, the latter pores are charged very quickly; the potential in them reaches the critical value so that the process of galvanostatic charging should be stopped. As a result, the fine pores with the large surface areas remain uncharged.

The highly disperse surface can be also charged in the potentiostatic mode; however, here, according to estimates, the flows of ions migrating to the active layer are limited. Estimates have shown that for the permissible potential difference of 1 V (aqueous electrolytes), it takes several tens of minutes rather than

Table 11. Dependence of the fraction of carbon grains in the active layer g on the parameters of potentiostatic charging process and its results, namely, the charging time t^* and specific volume values of capacitance C_{sp} and energy W_{sp}

g	κ^{***}, S cm^{-1}	S^{***}, cm^{-1}	R, μm	l, μm	n, cm^{-2}	t^*, s	C_{sp}, F/cm^3	W_{sp}, J/cm^3
0.65	0.108	1.18×10^7	5.67	10.03	2.48×10^5	5.317×10^{-4}	125.7	54.37
0.55	0.092	1.31×10^7	6.67	8.91	3.15×10^5	1.642×10^{-4}	90.38	39.39
0.45	0.0896	1.33×10^7	8.21	9.89	2.56×10^5	9.26×10^{-5}	64.97	28.40
0.35	0.088	1.355×10^7	16.93	17.33	8.32×10^4	5.124×10^{-6}	9.70	4.257

several seconds to charge the active layers of activated carbon several mm thick.

Thus, used separately, neither galvanostatic nor potentiostatic modes of charging the supercapacitor active layers can provide specific capacitances of several hundred F/g in several seconds and even several fractions of second. These values can be reached by alternating galvanostatic and potentiostatic modes. In this study, the method of combined charging of the active layer in two stages is considered. First, the galvanostatic mode is used and then, when the potentials in the active layer reach the maximum possible values, the charging continues in the potentiostatic mode.

For the two-step methods of charging of supercapacitor active layers we proposed, it is typical that the model of cylindrical electrolyte pores (Section 7) selected for calculating the overall characteristics of EDLC requires the knowledge of the following structural parameters of the activated carbon material used for preparation of EDLC active layers: the average radius of wide electrolyte pores ρ_2 and the average radius of fine electrolyte pores ρ_1 (actually, the variables are the structural parameters of the model shown in Fig. 1, D and d), and the fraction of material accounted for fine pores g. These three values are supplemented by two more parameters: the charging current density (galvanostatics) I and the active layer thickness L.

After this, we can embark on estimation of the following values: the galvanostatic stage time (designated as t_{gal}) and the potentiostatic stage time (t_{pot}). Furthermore, the following obvious criterion should be fulfilled: the time t_{gal} should be much smaller than the time t_{pot}. The fulfillment of the latter requirement ensures the reliability of results, the attainment of the minimum charging time of the active layer and the maximum overall characteristics of the EDLC.

APPENDIX 1

Derivation of Formulas for Overall Characteristics of EDLC (Galvanostatic Mode)

The calculation of overall characteristics of EDLC in the galvanostatic mode is based on determination of the potential distribution throughout the active layer thickness in arbitrary time intervals. The potential distribution can be found by solving the following equation [27]:

$$\kappa\frac{d^2E}{dx^2} = SC_s\frac{dE}{dt} \tag{A.1}$$

with boundary conditions $\frac{dE(0,t)}{dx} = 0$ and $\kappa\frac{dE(L,t)}{dx} = I$ and the initial condition $E(x,0) = E_0$.

The potential distribution has the following form:

$$E(x,t) = E_0 + \frac{I}{\kappa}L\left[\frac{t}{\tau} + \frac{3x^2 - L^2}{6L^2} + \frac{2}{\pi^2} \times \sum_{m=1}^{+\infty}(-1)^{m+1}\frac{\exp(-m^2\pi^2 t/\tau)}{m^2}\cos(m\pi x/L)\right], \tag{A.2}$$

where $\tau = \frac{L^2SC_s}{\kappa}$.

The time of capacitor charging in the galvanostatic mode is limited by the attainment of the maximum permissible potential in a certain point. Such critical point is the active layer boundary $x = L$. The charging time t^* is determined by the condition $E^* = E(L, t^*)$ or

$$\frac{I}{\kappa}L\left[\frac{t^*}{\tau} + \frac{1}{3} - \frac{2}{\pi^2}\sum_{m=1}^{+\infty}\frac{\exp(-m^2\pi^2 t^*/\tau)}{m^2}\right] = E^* - E_0.$$

The capacitor gains the charge $Q = It^*$. in time t^*. The charge distribution throughout the layer thickness can be characterized by the linear density $q(x,t)$, found from the equation

$$\frac{\partial q}{\partial t} = \kappa\frac{\partial^2 E}{\partial x^2}.$$

Substituting the latter equation into expression (A.2), we obtain

$$\frac{\partial q(x,t)}{\partial t} = I\left[\frac{1}{\tau} - \frac{2}{L}\sum_{m=1}^{\infty}(-1)^{m+1}\left\{\exp\left(-m^2\pi^2 t/\tau\right)\right\}\cos(m\pi x/L)\right].$$

After integration of the right part, we have

$$q(x,t) = I\left[\frac{t}{\tau} - \frac{\tau}{L}\frac{2}{\pi^2}\sum_{m=1}^{\infty}\frac{(-1)^{m+1}}{m^2} \times \left\{1 - \exp\left(-m^2\pi^2 t/\tau\right)\right\}\cos(m\pi x/L)\right]. \tag{A.3}$$

The energy contained in a layer with the thickness dx is equal to $dW(x, t) = q(x,t)\varphi(x,t)dx$.

Then, the energy of the EDLC active layer is calculated by integration

$$W(t) = \frac{1}{2}\int_0^L q(x,t)\varphi(x,t)dx.$$

As a result, we obtain that the time dependence of the energy stored in the EDLC active layer is described by the formula

$$W(t) = \frac{I^2}{2\kappa}\left\{\frac{Lt^2}{\tau} - \frac{L2\tau}{\pi^4}\sum_{m=1}^{\infty}\frac{\left[1 - \exp\left(-m^2\pi^2 t/\tau\right)\right]^2}{m^4}\right\}.$$

The specific volume energy is

$$W_{sp} = \frac{W(t)}{L} = \frac{I^2}{\kappa}\frac{\tau}{2}\left\{\frac{t^2}{\tau^2} - \frac{2}{\pi^4}\sum_{m=1}^{\infty}\frac{\left[1-\exp\left(-m^2\pi^2 t/\tau\right)\right]^2}{m^4}\right\}. \quad (A.4)$$

The specific volume power is

$$P_{sp}(t) = \frac{dW}{dt} = \frac{I^2}{k}\left\{\frac{t}{\tau} + \frac{2\tau}{\pi^2\tau} \times \sum_{m=1}^{\infty}\frac{\left[1-\exp\left(-m^2\pi^2 t/\tau\right)\right]}{m^2}\exp\left(-m^2\pi^2 t/\tau\right)\right\}. \quad (A.5)$$

The capacitance is calculated according to the formula

$$C(t) = \frac{Q(t)^2}{2W(t)} = \frac{\kappa t^2}{L\left\{\frac{t^2}{\tau} - \frac{2\tau}{\pi^4}\sum_{m=1}^{\infty}\frac{\left[1-\exp\left(-m^2\pi^2 t/\tau\right)\right]^2}{m^4}\right\}},$$

$$C_{sp}(t) = \frac{C(t)}{L} = \frac{\kappa t^2}{L^2\left\{\frac{t^2}{\tau} - \frac{2\tau}{\pi^4}\sum_{m=1}^{\infty}\frac{\left[1-\exp\left(-m^2\pi^2 t/\tau\right)\right]^2}{m^4}\right\}}.$$

The capacitance at $t \to \infty$ is

$$C_{sp}(t) \to \frac{\kappa t^2}{L^2\left\{\frac{t^2}{\tau}\right\}} = \frac{\kappa\tau}{L^2} = \frac{\kappa\frac{L^2 SC_s}{\kappa}}{L^2} = SC_s.$$

APPENDIX 2

Derivation of Formulas for Overall Characteristics of EDLC (Potentiostatic Mode)

I. The potential distribution near an electrolyte pore is found by solving the equation

$$\kappa\left\{\frac{\partial^2 E(r,t)}{\partial r^2} + \frac{1}{r}\frac{\partial E(r,t)}{\partial r}\right\} = SC_s\frac{\partial E(r,t)}{\partial t},$$
$$r_1 < r < r_2, \quad 0 < t < +\infty, \quad r_2 = l$$

with boundary conditions $E(r_1,t) = E^*$, $\frac{\partial E}{\partial r}(r_2,t) = 0$ and initial condition $E(r, 0) = E_0$.

This solution has the form

$$E(r,t) = E^* + (E^* - E_0) \times \pi\sum_{m=1}^{\infty}\frac{J_1(\mu_m)J_0\left(\mu_m\frac{r_1}{r_2}\right)}{\left[J_0\left(\mu_m\frac{r_1}{r_2}\right)\right]^2 - \left[J_1(\mu_m)\right]^2} \times e^{-\mu_m^2 t/\tau}\left\{J_1(\mu_m)N_0\left(\mu_m\frac{r}{r_2}\right) - N_1(\mu_m)J_0\left(\mu_m\frac{r}{r_2}\right)\right\}, \quad (B.2)$$

where $J(r)$ and $N(r)$ are the Bessel function of the 1st and 2nd orders, respectively [28, 29],

$$\tau = \frac{SC_s r_2^2}{\kappa},$$

and μ_m are positive roots of the following equation:

$$J_0\left(\mu_m\frac{r_1}{r_2}\right)N_1(\mu_m) - N_0\left(\mu_m\frac{r_1}{r_2}\right)J_1(\mu_m) = 0. \quad (B.3)$$

Actually, the process of potentiostatic charging should be carried out not in the infinite time when the potential becomes constant throughout the thickness of the highly disperse layer between two cylindrical surfaces but in the finite time t^* corresponding to the moment when the potential on the back cylindrical surface ($r = r_2$) reaches a value $E(r_2, t^*) = \eta E^*$ (where parameter η is confined in interval $0.9 \le \eta \le 1$) lower than E^* albeit quite acceptable.

The dependence of the real charging time t^* on parameter η can be found by solving the following equation:

$$\eta E^* = E^* - (E^* - E_0) \times \sum_{m=1}^{\infty}\frac{J_1(\mu_m)J_0\left(\mu_m\frac{r_1}{r_2}\right)}{\left[J_0\left(\mu_m\frac{r_1}{r_2}\right)\right]^2 - \left[J_1(\mu_m)\right]^2}e^{-\mu_m^2 t^*/\tau}\frac{2}{\mu_m}. \quad (B.4)$$

II. The charge accumulated in supercapacitor micropores.

Charges enter the micropores through the walls of a macropore. The current that flows though walls of an individual cylindrical macropore (with the radius $r_1 = R$) is

$$I_1(t) = 2\pi r_1 L\left(-\kappa\frac{\partial E}{\partial r}_{r=r_1}\right) = 2\pi r_1\kappa(E^* - E_0)\sum_{m=1}^{\infty}\frac{J_1(\mu_m)^2}{J_0\left(\mu_m\frac{r_1}{r_2}\right)^2 - J_1(\mu_m)^2}e^{-\mu_m^2 t/\tau}\frac{2}{r_1}.$$

The total current that flows from all (n) macropores into the carbon medium (through the surface of cylinders of the unit length $L = 1$) is

$$I(t) = nI_1 = 4n\pi\kappa(E^* - E_0) \times \sum_{m=1}^{\infty} \frac{J_1(\mu_m)^2}{J_0\left(\mu_m \frac{r_1}{r_2}\right)^2 - J_1(\mu_m)^2} e^{-\mu_m^2 t/\tau}. \quad \text{(B.5)}$$

Assume that charging of a supercapacitor proceeds in time t^* up to the moment where the potential at $r = r_2$ turns out to be $E(r_2, t^*) = \eta E^*$, where $0.9 \le \eta \le 1$.

In time $t \le t^*$, the following charge is accumulated on the supercapacitor:

$$Q(t) = \int_0^t I(t)dt = n4\pi r_2^2 SC_s(E^* - E_0) \times \sum_{m=1}^{\infty} \frac{J_1(\mu_m)^2}{J_0(\mu_m r_1/r_2)^2 - J_1(\mu_m)^2} \frac{1 - e^{-\mu_m^2 t/\tau}}{\mu_m^2}. \quad \text{(B.6)}$$

III. The energy of a supercapacitor is calculated by the formula

$$W(t) = \frac{1}{2}\int_{r_1}^{r_2} q(r,t)(E(r,t) - E_0)2\pi r dr,$$

where $q(r, t)$ is the charge density. The charge density is proportional to the specific capacitance and the potential in the point under consideration. The dependence of the charge density on coordinates and time is

$$q(r,t) = SC_s(E(r,t) - E_0) = SC_s(E^* - E_0) \times \left\{1 - \pi\sum_{m=1}^{\infty} B_m R_m(r)\exp(-\mu_m^2 t/\tau)\right\},$$

where

$$R_m(r) = \left\{J_1(\mu_m)N_0\left(\frac{\mu_m r}{r_2}\right) - N_1(\mu_m)J_0\left(\frac{\mu_m r}{r_2}\right)\right\},$$

$$B_m = \frac{J_1(\mu_m)J_0\left(\frac{\mu_m r_1}{r_2}\right)}{\left[J_0\left(\frac{\mu_m r_1}{r_2}\right)\right]^2 - \left[J_1(\mu_m)\right]^2}.$$

Taking into account equality (B.5), we rewrite the expression for energy as follows:

$$W(t) = \frac{SC_s(E^* - E_0)^2}{2} \times \int_{r_1}^{r_2}\left\{1 - \pi\sum_{m=1}^{\infty} B_m R_m(r)\left[1 - \exp\left(-\mu_m^2 t/\tau\right)\right]\right\}^2 2\pi r dr.$$

As a result of integration with due regard to the orthogonality of the eigenfunctions $R_m(r)$ in the segment $r_1 \le r \le r_2$, we obtain

$$W(t) = n\pi(E^* - E_0)^2 SC_s \frac{r_2^2}{2}\left\{1 - \frac{r_1^2}{r_2^2} + 4\sum_{m=1}^{\infty} \frac{\left[J_1(\mu_m)\right]^2 \exp(-2\mu_m^2 t/\tau) - 2\exp(-\mu_m^2 t/\tau)}{\left[J_0(\mu_m r_1/r_2)\right]^2 - \left[J_1(\mu_m)\right]^2} \frac{1}{\mu_m^2}\right\}. \quad \text{(B.7)}$$

IV. Specific capacitance due to diffusion of ions into carbon grains

$$C_{sp} = \frac{Q(t)^2}{2W(t)} = \frac{n\pi r_2^2 SC_s\left[4\sum_{m=1}^{\infty} \frac{J_1(\mu_m)^2}{\left(J_0(\mu_m r_1/r_2)^2 - J_1(\mu_m)^2\right)} \frac{1 - \exp(-\mu_m^2 t/\tau)}{\mu_m^2}\right]^2}{\left\{1 - \frac{r_1^2}{r_2^2} + 4\sum_{m=1}^{\infty} \frac{\left[J_1(\mu_m)\right]^2}{\left[J_0(\mu_m r_1/r_2)\right]^2 - \left[J_1(\mu_m)\right]^2} \frac{\exp(-2\mu_m^2 t/\tau) - 2\exp(-\mu_m^2 t/\tau)}{\mu_m^2}\right\}}. \quad \text{(B.8)}$$

LIST OF PARAMETERS CHARACTERIZING THE ACTIVE LAYER OF A BIPOROUS CARBON EDLC

Parameters of Carbon Grains and Electrolyte Grains

D is the length of edges of cubic grains (carbon and electrolyte) in the active layer

$d = 1$ nm is the length of edges of cubic carbon particles in carbon grains

$S = S^*/d = 1.359 \times 10^7$ cm^{-1} is the specific surface of carbon particles in carbon grains

$g^{**} = 0.5$ is the volume concentration of carbon particles in carbon grains

$C_s = 2 \times 10^{-5}$ F/cm^2 is the specific capacitance of the electric double layer on the carbon material

Parameters of the Active Layer

$N_s = 100$ is the number of grains on model cube edges (the model cube volume is 10^6, i.e., one million of grains of two types)

L (cm) is the active layer thickness

x is the coordinate in the active-layer ($0 \le x \le L$)

$x^* = x/L$ is the normalized coordinate in the active layer ($0 \le x^* \le 1$)

$E(x, t)$ (V) is the potential in the active layer

$E(x, t = 0) = E_0$ (V) is the initial potential of the active layer

E^* (V) is the maximum possible potential in the active layer

t is the charging time

$t^* = t/\tau$ is the normalized charging time

$a = SC_s = 272$ F/cm^3 is the characteristic specific capacitance of carbon grains

ρ_2 is the average radius of wide pores in the active layer

ρ_1 is the average radius of fine pores in the active layer

C_{sp} (F/cm^3) is the specific volume capacitance of the active layer

W_{sp} (J/cm^3) is the specific volume energy of the active layer

Characteristics of the Aqueous Electrolyte Conductivity

$\kappa_0 = 0.8$ S cm^{-1} (30% H_2SO_4 + water) [30] is the specific conductivity of ions in electrolyte

κ^{**} is the normalized effective specific conductivity of ions in the active layer

$\kappa = \kappa_0\kappa^{**}$ (S cm^{-1}) is the effective specific conductivity of ions in the active layer

κ^{***} (S cm^{-1}) is the effective ionic conductivity of the highly disperse layer

Parameters of Percolation Clusters

g is the volume concentration (fraction) of carbon grains in the active layer

g^* is the ratio of grains within an electronic cluster

$g - g^*$ is the ratio of grains uninvolved in the electronic cluster

g_i is volume concentration (fraction) of electrolyte grains in the active layer

g_i^* is the ratio of grains involved in the ionic cluster

$g_i - g_i^*$ is the ratio of grains uninvolved in the ionic cluster

$g_i^{**} = g_i^* + (g - g^*)$ is the concentration of grains characterizing the effective ionic cluster

$\alpha = g^*/[g^* + (g_i - g_i^*)]$ is the degree of dilution of carbon grains in the highly disperse layer

$g^{***} = 0.298$ is the percolation threshold for the electronic cluster

$g_i^{***} = 0.298$ is the percolation threshold for the ionic cluster

$S^* = S/D$ is the normalized specific surface of the contact between electronic and ionic clusters

$S^{**} = S/D$ (cm^{-1}) is the specific surface of the contact between electronic and ionic clusters

Parameters of Galvanostatic Charging

I (A/cm^2) is the charging current density

t_{gal} is the time of galvanostatic process

$\tau = SC_sL^2/\kappa$ is the characteristic charging time

C (F/cm^2) is the specific capacitance of the active layer

C/L (F/cm^3) is the specific volume capacitance of the active layer

W (J/cm^2) is the specific energy of the active layer

W/L (J/cm^3) is the specific volume energy of the active layer

Parameters of the Model of Cylindrical Electrolyte Pores

R is the radius of cylindrical pores

n is the number of cylindrical electrolyte pores per cm^2 of the active layer surface

l is the half-distance between neighboring cylindrical pores

Parameters of the Potentiostatic Charging Mode

t_{pot} is the time of potentiostatic process

$r_1 = R$ is the polar radius of the front surface of the highly disperse layer

$r_2 = l$ is the polar radius of the back surface of the highly disperse layer

S^{***} (cm^{-1}) is the specific surface of carbon in the highly disperse layer

η is the degree of charging of the highly disperse layer

$\psi = [4l^2 - \pi R^2]/[\pi (l^2 - R^2)]$ is the coefficient of gain of the highly disperse part of the active layer

REFERENCES

1. Conway, B.E., *J. Electrochem. Soc.*, 1991, vol. 138, p. 1539.
2. Vol'fkovich, Yu.M. and Serdyuk, T.M., *Russ. J. Electrochem.*, 2002, vol. 38, p. 935.
3. Pillay, B. and Newman, J., *J. Electrochem. Soc.*, 1996, vol. 143, p. 1806.
4. Lin, C., Ritter, J.A., Popov, B.N., and White, R.E., *J. Electrochem. Soc.*, 1999, vol. 146, p. 3168.
5. Vol'fkovich, Yu.M., Mazin, V.M., and Urisson, N.A., *Russ. J. Electrochem.*, 1998, vol. 34, p. 740.
6. Fialkov, A.S., *Russ. J. Electrochem.*, 2000, vol. 36, p. 345.
7. *New Carbon Based Materials for Electrochemical Energy Storage Systems: Batteries, Supercapacitors and Fuel Cells*, Barsukov, I.V., Johnson, C.S., Doninger, J.E., and Barsukov, V.Z., Eds., Dordrecht: Springer, 2006.
8. Rychagov, A.Yu., *Extended Abstract of Cand. Sci. (Chem.) Dissertation*, Moscow, 2008.
9. Simon, P. and Gogotsi, Y., *Phil. Trans. R. Soc. A*, 2010, vol. 368, p. 3457.

10. Sing, K.S.W., Everett, D.H., Haul, R.A.W., Moscou, L., Pierotti, R.A., Rouquerol, J., and Siemieniewska, T., *Pure Appl. Chem.*, 1985, vol. 57, p. 603.
11. Frackowiak, E. and Beguin, F., *Carbon*, 2001, vol. 39, p. 937.
12. Halper, M.S. and Ellenbogen, J.C., in *MITRE Nanosystems Group 1 (March)*, 2006, p. 1.
13. Pandolfo, A.G. and Holltenkamp, A.F., *J. Power Sources*, 2006, vol. 157, p. 11.
14. Wang, G., Zhang, L., and Zhang, J., *Chem. Soc. Rev.*, 2012, vol. 41, p. 797.
15. de Levie, R., *Electrochim. Acta*, 1963, vol. 8, p. 751.
16. de Levie, R., *Electrochim. Acta*, 1964, vol. 9, p. 1231.
17. Posey, F.A. and Morozumi, T., *J. Electrochem. Soc.*, 1966, vol. 113, p. 176.
18. Chizmadzhev, Yu.A., Markin, V.S., Tarasevich, M.R., and Chirkov, Yu.G., *Makrokinetika protsessov v poristykh sredakh (Toplivnye elementy)* (Macrokinetics of Processes in Porous Media (Fuel Cells)), Moscow, 1971.
19. Fenelonov, V.B., *Poristyi uglerod* (Porous Carbon), Novosibirsk, 1995.
20. Karnaukhov, A.P., *Adsorbtsiya. Tekstura dispersnykh i poristykh materialov* (Adsorption. Texture of Disperse and Porous Materials), Novosibirsk, 1999.
21. Chirkov, Yu.G. and Rostokin, V.I., *Russ. J. Electrochem.,* 2014, vol. 50.
22. Chirkov, Yu.G. and Rostokin, V.I., *Russ. J. Electrochem.*, 2003, vol. 39, p. 622.
23. Tarasevich, Yu.Yu., *Perkolyatsiya: teoriya, prilozheniya, algoritmy* (Percolation: Theory, Applications, Algorithms), Moscow: Editorial URSS, 2001.
24. Chirkov, Yu.G., *Russ. J. Electrochem.*, 1999, vol. 35, p. 1281.
25. Chirkov, Yu.G., Rostokin, V.I., and Skundin, A.M., *Russ. J. Electrochem.*, 2011, vol. 47, p. 71.
26. Chirkov, Yu.G. and Rostokin, V.I., *Russ. J. Electrochem.,* 2006, vol. 42, p. 715.
27. Daniel'-Bek, V.S., *Zh. Fiz. Khim.*, 1948, vol. 22, p. 697.
28. Tikhonov, A.N. and Samarskii, A.A., *Uravneniya matematicheskoi fiziki* (Equations of Mathematical Physics), Moscow: MGU, Nauka, 2004.
29. Goryunov, A.F., *Uravneniya matematicheskoi fiziki v primerakh i zadachakh* (Equations of Mathematical Physics in Examples and Problems), Moscow: MIFI, 2008.
30. Darling, H.E., *J. Chem. Eng. Data*, 1964, vol. 9, p. 421.

Translated by T. Safonova